INT. J. REMOTE SENSING, 2003, VOL. 24, NO. 3, 595–609

Validation of urban boundaries derived from global night-time satellite imagery

M. HENDERSON*†, E. T. YEH‡, P. GONG†, C. ELVIDGE§ and K. BAUGH¶

†Department of Environmental Science, Policy, and Management, University of California, Berkeley, CA 94720-3312, USA
‡Energy and Resources Group, University of California, Berkeley, CA 94720-3050, USA
§National Geophysical Data Center, US National Oceanographic and Atmospheric Administration, 325 Broadway, Boulder, CO 80303, USA
¶Cooperative Institute for Research in Environmental Sciences, University of Colorado, Boulder, CO 80303, USA

(*Received 1 November 2000; in final form 19 November 2001*)

Abstract. Night-time imagery from the Defense Meteorological Satellite Program (DMSP) Operational Linescan System (OLS) has been proposed as a useful tool for monitoring urban expansion around the world, but determining appropriate light thresholds for delineating cities remains a challenge. In this paper we present a new approach. We used DMSP stable lights and radiance-calibrated images to delimit urban boundaries for San Francisco, Beijing and Lhasa, cities with different levels of urbanization and economic development, and compared the results against boundaries derived from high-resolution Landsat Thematic Mapper (TM) imagery. Unthresholded DMSP images exaggerate and shift the extent of these urban areas. We then calculated light thresholds that minimized the discrepancies between the DMSP- and TM-derived urban boundaries for each city. Our comparison highlights the difficulty of using DMSP data across areas with disparate urban characteristics, but suggests the possibility of calibrating this data source for monitoring growth of cities at comparable levels of development.

1. Introduction

Urban areas are expanding rapidly in many parts of the world. Urban encroachment upon agricultural and forest lands often leads to environmental degradation and a loss of natural productivity, leading some analysts to suggest that the present rate of urbanization constitutes a global crisis (Dickenson 1975, Krohe 1986, Brown 1995). In much of the world, however, it is difficult to measure accurately rates of urban growth. Even in the United States and Europe, urbanized unincorporated areas are not always included in formal census entities designated as 'urban', and 10-year time intervals between censuses may not be sufficient for monitoring rapid rates of urban growth (Imhoff *et al.* 1997a).

*Corresponding author; e-mail: mhenders@nature.berkeley.edu

International Journal of Remote Sensing
ISSN 0143-1161 print/ISSN 1366-5901 online © 2003 Taylor & Francis Ltd
http://www.tandf.co.uk/journals
DOI: 10.1080/01431160210144534

Satellite remote sensing has long been a useful alternative for mapping the expansion of urban land uses. However, common approaches remain problematic. Imagery from fine-resolution sensors such as Landsat or Système Probatoire de l'Observation de la Terre (SPOT) provides a level of detail sufficient to distinguish urban from non-urban land uses in most cases. Unfortunately these sources are too expensive for most university researchers to acquire and process at continental to global scales. Imagery from coarser resolution sensors such as the Advanced Very High Resolution Radiometer (AVHRR; with pixel size 1 km^2 or greater) is better suited to wide-scale, frequently repeated surveys of land use change (NOAA 2001). However, AVHRR is not optimally suited for detecting cities because of its coarse resolution.

Landsat, SPOT and AVHRR sensors are for the most part designed to detect reflected solar radiation; thus, they collect imagery during daytime. But urban areas in modern societies are brightly lit at night, making it much easier to distinguish them from surrounding non-urban lands at night-time. The Defense Meteorological Satellite Program's Operational Linescan System (DMSP OLS; hereafter DMSP) collects imagery at night and has a number of unique features that meet the needs of wide-scale, frequently repeated surveys of urban growth. The DMSP platform follows a Sun-synchronous orbit at a nominal altitude of 830 km while its pendulum-type analog sensor is sampled at a constant rate as it sweeps across a 3000 km swath. In its high-resolution mode this produces images with pixels whose ground locations are a roughly equidistant 500 m apart at nadir (NOAA 1999) and slightly over 1 km at the edge of the swath. The platform's 101-min orbital period allows it to cross any point on the earth at least once daily (twice at higher latitudes). Most notable is the DMSP sensor's capability to detect even very low levels of visible and near-infrared light (0.40–1.10 μm) emitted from urban and other terrestrial sources, as detailed below. Working on the premises that lit areas are (for the most part) urban areas, and that the intensity of cities' night-time lighting is proportional to their population and level of economic development, Elvidge *et al.* (1997a, b, 1999), Imhoff *et al.* (1997a, b), Sutton (1997), Sutton *et al.* (1997, 1999a, b) and others have used DMSP night-time satellite imagery to detect and analyse the extent and density of urban settlements.

Elvidge *et al.* (1998) processed raw DMSP imagery to produce two composite images covering the globe. The 'stable lights' image depicts the stability of light sources from October 1994 to March 1995, with transient lights (visible on fewer than 6% of cloud-free orbits) filtered out. The 'radiance-calibrated' image depicts the maximum intensity of light from each source over the months of March 1996 and January and February 1997. Both composite images are resampled down to a resolution of 1 km, comparable to AVHRR 1.1 km imagery. To date most research has used the stable lights imagery, which has been shown to correlate with US urban population density (Sutton *et al.* 1997), and thus to be useful in a variety of applications including the area of urbanization in the US and its potential impact on soil resources (Imhoff *et al.* 1997b). Sutton *et al.* (1999a) also sought to estimate the global human population using this data source. More recently, Elvidge (2000b) has explored the utility of the radiance-calibrated image in detecting low-density human settlements.

A major challenge for researchers applying DMSP imagery to delineate urban areas is choosing appropriate thresholds. Previous work has attempted to validate DMSP-derived urban boundaries by comparing them to population densities reported on census maps (Imhoff *et al.* 1997a) or subnational statistics on urban populations (Sutton *et al.* 1999a). In this paper we present a new approach, validating

DMSP-derived urban boundaries against higher resolution Landsat TM imagery. We examine three urban areas as they appear in both composite DMSP images—the stable lights and radiance-calibrated images—and in Landsat imagery for approximately the same dates. While daytime Landsat imagery is most commonly used for differentiating among geomorphological features and types of vegetation cover, it has also been used to detect urban areas and measure their change over time (e.g. Lo and Welch 1977, Lo *et al.* 1977, Coulter and Ivory 1982). Such high-resolution imagery is admittedly impractical for mapping urbanization with high temporal frequency and wide geographic coverage, but it offers a useful benchmark for testing the application of DMSP imagery to this purpose.

We find that, relative to the Landsat analysis, the DMSP data tend to exaggerate the size of the urban areas, whether due to reflectance of light from surrounding water and non-urban land areas, to physical properties of the sensor, or to the cumulative effects of georeferencing errors made in the capture and compositing of DMSP imagery. Our objective is to contribute to the development of rules for deriving more accurate urban boundary information from DMSP composite imagery. If such rules can be developed, DMSP imagery will be more useful in monitoring the rate of urbanization around the globe.

2. Study areas

We performed analyses for three cities representing different degrees of urbanization and development.

2.1. *Lhasa*

Lhasa is the smallest and least developed of the cities we examined. The city of Lhasa is located in the southern part of the Tibetan plateau (29°39′N 91°06′E) at an altitude of 3600 m above sea level. The valley in which Lhasa lies is formed by the Kyichu River, a tributary of the Yarlung Tsangpo (which becomes the Brahmaputra in India). The peaks surrounding Lhasa range between 4400–5300 m, but the city itself is built on a plain of marshy grounds around three small hills. The Lhasa valley is sheltered from harsh winds and has a much more moderate climate than the surrounding plateau. Maximum summer daytime temperatures are around 28°C, whereas wintertime lows are around −15°C. Average precipitation is only around 450 mm y^{-1}, with 90% falling between July–September. The city enjoys over 300 days of sunshine per year (Alexander and de Azevedo 1998). Although some ecologists believe that the hills surrounding Lhasa were covered with juniper trees 1000 years ago, the surrounding hills now are covered only with grass during the rainy season and are largely barren during the rest of the year.

Lhasa has been the capital of Tibet and the religious centre of Tibetan civilization since the seventh century AD. In 1948, the city's population was approximately 30 000. Population estimates for Lhasa in the late 1990s range from 200 000–400 000, but these may not include the large presence of temporary migrants and military personnel in the city. Rapid growth occurred only after restrictions on internal migration in China were relaxed in the 1980s, and the most rapid expansion in both city area and population has taken place since 1992. Industrial production is limited to a few cement plants and carpet factories. The economy of Lhasa itself rests largely on government inputs and the service sector. In the surrounding countryside, areas below 4200 m are used for farming barley, wheat, beans and rapeseed; areas above 4200 m are pastoral.

2.2. *Beijing*

Beijing, capital city of China, is one of its largest and most developed urban areas. The city is strategically located on the western edge of the North China Plain (40°15′ N 116°30′ E) at an elevation of 45 m, about 200 km inland from the port of Tianjin. Within 50 km north and west of the city, the Taihang and Jundu mountains, straddled by the famed Great Wall, rise to heights of 2300 m. As winter winds descend from Siberia, the city's temperature drops from a summertime high of 26°C to lows of −20°C in the depths of winter. In spring, the winds shift to blast the city with fine yellow dust particles from the Loess Plateau and central Asia. Summer is the rainy season.

Beijing's history as a capital city dates as far back as China's Warring States period (484–221 BCE). Most significantly, it was the centre of the Mongols' east Asian empire at the time of Marco Polo (*ca* 1285) and was the capital of the Ming and Qing dynasties (1368–1643 and 1644–1911). At the establishment of the People's Republic of China in 1949, the city was again made the national capital. Beijing has experienced more constant expansion over the past five decades than any other Chinese city. Qing city walls were replaced with ring roads, multi-storey housing blocks rose over the alleys of the old city, and surrounding villages became suburbs in a conurbation with some 6.5 million residents by 2000. (Beijing municipality, encompassing 10 counties as well as the central city area, reports a population of 12 million.) Since the beginning of economic reforms in 1978, development of the surrounding countryside has been especially brisk. The plains east and south of the city are now a chequerboard of high-intensity agricultural lands and new urban areas, while nearby mountainous areas, though targets of reforestation since the 1960s, also show the effects of economic expansion.

2.3. *San Francisco*

San Francisco, on the California coast (37°46′ N 122°25′ W), represents a highly developed urban area in the US. The Landsat imagery used in this evaluation includes the city of San Francisco itself along with portions of the contiguous urban areas of Alameda and Marin counties. San Francisco Bay is the most prominent feature in the scene. Winter brings almost all of the region's precipitation—about 525 mm y^{-1}—but the summer months are most susceptible to San Francisco's famous thick coastal fog. Hills ring the Bay; Mount Tamalpais, at the edge of our study area, rises to a height of over 700 m.

The San Francisco region saw its first European settlement in 1776, starting with the establishment of Mission Dolores by the Spanish. Rapid urbanization began with arrival of Americans and many others from around the world in the gold rush of 1849. The urban areas within our study area were fully developed by the 1960s, while the urban boundary of the San Francisco Bay area continues to expand beyond the nine counties that ring the Bay. Technological and economic change have altered the industrial composition of our study area. San Francisco's port has withered, replaced in importance by high-technology service companies, while across the Bay (and also within our study area) the Port of Oakland has modernized to maintain its position as the third largest port on the Pacific Coast of the US.

3. Methods

For each of the three cities, we began by coregistering DMSP and Landsat TM data, delineating urban land uses in the Landsat images, and generating urban

boundaries from the two types of DMSP images using three different classification thresholds each. These steps are detailed here.

3.1. *Coregistering Landsat TM and DMSP data*

We made use of available Landsat 5 images that were reasonably close in date to the mid-1990s time frame of the DMSP composite imagery. For Lhasa, we used a portion of a scene from January 1989; for San Francisco, a portion of a scene from July 1990; and for Beijing, a portion of a scene from August 1994. Fortunately, the acquisition date of the image for the fastest-growing of our urban areas (Beijing) is very close to the dates of the DMSP data. The images were system-corrected by the US Geological Survey EROS (Earth Resource Observation Systems) Data Center. We georeferenced these images into UTM (Universal Transverse Mercator) projections using nearest neighbour resampling to ground control points that were visible on both the Landsat images and on the best available Geographical Information System (GIS) vector datasets available to us. For San Francisco, these were shoreline points and road intersections from US Geological Survey 1:24 000 topographic maps (available as 1:100 000 digital line graphs). For Beijing and Lhasa, we used rivers and highways from the 1:1 000 000 Digital Chart of China (CIESIN 1996). We recognize that these sources for ground control points are imperfect. While the San Francisco vector data are relatively reliable, we could at best expect a georeferencing error of ± 60 m. The Beijing and Lhasa vectors are putatively accurate only to within 650 m on the ground, and a comparison with other map sources suggests that figure may be overly optimistic. However, in comparing these errors to the size of the DMSP pixels (composited at 1 km on a side), we see that the relative error is small for our purposes.

Since we had obtained complete Landsat scenes (measuring 185 km on a side) for Beijing and Lhasa, we extracted a smaller area from each of these scenes containing the entire contiguous built-up area and extending 20 km or more into the surrounding countryside. In the case of San Francisco, the image file available to us had already been clipped to focus on a small portion of the larger San Francisco–Oakland–San Jose conurbation. Our subsequent analysis focused on these study areas. To bring the DMSP imagery into the same spatial framework as our Landsat study areas, we extracted three small rectangles from the global images and reprojected them into the UTM projections used above, simultaneously resampling the DMSP imagery from its 1 km resolution to the 30 m resolution of the Landsat TM data. It should be noted that while the georeferencing of the original DMSP images is very good (± 1 pixel), they are known to display a slight bias toward the north.

3.2. *Delineating urban lands in the Landsat TM data*

We identified urban lands in our study areas by performing the commonly used supervised maximum likelihood classification on each (Ding *et al.* 1998). Performing this classification without the use of *a priori* probabilities, we initially produced as many as 20 classes of land cover. We then drew on our knowledge of the study areas and additional published maps to merge these classes into urban and non-urban land use classes. In the San Francisco study area, the landscape is clearly dominated by high-density urban areas, forested hillsides and the San Francisco Bay. The Beijing study area represented a more complex environment: the high-density urban area is surrounded by a patchwork of agricultural settlements as well as farmland, forested

hillsides and reservoirs. Finally, we found it difficult to distinguish Lhasa's small urban area from the surrounding barren mountains relying only on spectral characteristics. To improve the delineation of an urban boundary we applied a masking technique to exclude barren slopes because they exhibit spectral characteristics very similar to many urban surfaces. Following classification of the three images into multiple land cover classes, we extracted from each study site only the urban land use classes into new images.

3.3. *Processing the DMSP night-time lights data*

Operation of the DMSP is described by Elvidge *et al.* (1997a,b, 1998, 1999). Elvidge *et al.* (1997a) generated composite data files in the two formats introduced above. The stable lights image used in this study was produced from a composite of approximately 180 orbits between October 1994–March 1995. Pixel values in this file correspond to the percentage of time any light was seen, relative to the total number of cloud-free observations. Pixels in which light was observed on fewer than 6% of orbital passes were considered noise and removed from the dataset. Lights that appeared in ocean areas were classified as fishing-boat lights. Onshore lights that appeared for only a few weeks were classified as forest fires (these were widespread around the world in 1994–95). The remaining stable lights were attributed to urban areas.

Whereas the stable lights image provides no indication of the brightness of the lights, digital numbers (DNs) in the radiance-calibrated image are a function of the maximum intensity of light in the sensor's visible to near-infrared band (radiance = $DN^{3/2} \times 10^{-10}$ W cm^{-2} sr^{-1} μm^{-1}) observed in each pixel over several orbital passes in three months of 1996 and 1997. For these months, the sensor alternated between low-gain and high-gain settings, effectively extending the capabilities of the sensor to distinguish intensities of light. The high-gain setting offers better success at detecting artificial lighting in sparsely populated rural settings, while the low-gain setting allows for the better differentiation of light intensities within bright urban core areas. In the creation of this composite image the DNs have been calibrated so that values can be compared across dates and settings (Elvidge and Baugh 1998, Elvidge *et al.* 1999).

From the outset it was clear that the lit areas seen in the DMSP images around all three cities were much larger than the urban land use areas derived from our Landsat TM imagery. There are several reasons to expect this to be the case. First, the pixels in the DMSP composite images are approximately 1000 times larger than the TM pixels. This causes subpixel light sources to expand up to the larger DMSP pixel size. Second, atmospheric effects can also contribute to the spread in lights. Raw DMSP images containing cold clouds were not used in the production of the stable lights and radiance-calibrated composites, but warmer atmospheric phenomena (fog or air pollution) could not be excluded. Finally, these effects are compounded as geo-referencing errors are accumulated through a time series of observations in the compositing process.

However, the overly large lit areas seen at first glance in the DMSP images include all of the pixels that surpass only the *lowest* of thresholds—showing only the lowest level of detectable light in the radiance-calibrated image, or showing light during as few as 6% of the orbital passes represented in the stable lights image. Higher thresholds would yield urban areas more comparable in size to those delineated from Landsat TM imagery. Working with the stable lights image, Sutton *et al.*

(1997) found that 8% of the US land area was lit in 100% of orbital passes and an additional 3% was lit with less frequency (thresholds from 99% down to 6%). Subsequently, Sutton *et al.* (1999a) suggested using a threshold value of 80% based on their comparison of data on population and lit area for cities from a number of high, middle and low income countries.

Our approach here was to generate 'urban boundaries' from DMSP imagery using three different thresholds. The size and shape of these boundaries were then compared with the urban land use areas derived by conventional means from our Landsat TM imagery. For the stable lights images, we used the minimum threshold of 6% and a second threshold of 80% as used by Sutton *et al.* (1999a). For the radiance-calibrated images, we used the minimum level of detectable light (10^{-10} W cm^{-2} sr^{-1} μm^{-1}, or DN $\geqslant$ 1) and a second threshold of 8.94^{-9} W cm^{-2} sr^{-1} μm^{-1} (DN $\geqslant$ 20), approximating the land area lit at the 80% stable lights threshold. For both stable lights and radiance-calibrated images, we also calculated an 'optimum threshold' for each city such that the lit area at that threshold most closely matched the number of urban land use pixels in our classified Landsat TM imagery. We applied these thresholds to produce six different DMSP-derived 'urban boundaries' images for comparison with our Landsat TM-derived urban land use data.

4. Results and analysis for each city

Using the TM-derived urban land use classes as a standard, we performed an accuracy assessment on the six DMSP-derived urban boundaries images to produce confusion matrices summarizing how the TM and DMSP methods agree and disagree. We also compared the overall land area falling within the DMSP-derived urban boundaries with the TM-derived areas and, to draw attention to differences in shape and position, measured the linear distances and directional shift between them. The results of these comparisons are summarized in table 1 and figure 1. Details for each city follow.

4.1. *Lhasa*

Using a 1989 Landsat TM image of Lhasa we delineated an urban area of about 25 km^2. At the 6% and 80% thresholds, the DMSP stable lights imagery exaggerated the area by factors of 8.3 and 1.8, respectively. A threshold of 88% produced an area of the same size observed in the Landsat TM image, but the lit area at this threshold was shifted as much as 4 km north into barren mountains. DMSP radiance-calibrated imagery at the DN $\geqslant$ 1 threshold exaggerated the size of the urban area by a factor of 5.53, but the DN $\geqslant$ 20 threshold understated the urban area by one third. Adjusting slightly to a threshold of DN $\geqslant$ 19 (radiance = 8.28^{-9} W cm^{-2} sr^{-1} μm^{-1}) produced the target of 25.35 km^2, with somewhat less northward shifting observed. The shifting reduces the agreement in classification of the Landsat and DMSP sources (see tables 2 and 3).

These results show some of the difficulties in using DMSP imagery to delineate the urban area of a small, less developed city such as Lhasa. Reflectivity of night-time lights from the mountain sides north of Lhasa, may contribute to the exaggeration (the largest seen among our three cities) at lower thresholds. Although the radiance-calibrated image has been used to detect population densities as low as 16 people km^{-2} in the more developed setting of the US (Elvidge *et al.* 1999), the small villages in the vicinity of Lhasa do not register at all in this image, and the city itself is best detected at the low threshold of DN $\geqslant$ 19. Compounded geo-referencing errors

Table 1. Summary comparison of TM-derived urban areas with night-time lights imagery.

	Lhasa	Beijing	San Francisco
Landsat TM-derived urban area (km^2)	25.35	663	263
Lit area at DMSP stable lights threshold of 6% (km^2)	211	2936	968
Lit area at DMSP stable lights threshold of 80% (km^2)	45.9	1186	676
Optimal DMSP stable lights threshold (to produce a lit area comparable to the Landsat-derived urban area)	88%	97%	92%
Lit area at DMSP radiance-calibrated threshold of $DN \geqslant 1$ (km^2)	140	6430	788
Lit area at DMSP radiance-calibrated threshold of $DN \geqslant 20$ (km^2)	16.36	1402	616
Optimal DMSP radiance-calibrated threshold (to produce a lit area comparable to the Landsat-derived urban area)	$DN \geqslant 19$	$DN \geqslant 30$	$DN \geqslant 51$
Distance from TM-derived urban boundary to edge of stable lights at optimal threshold (km)	1.6–4.2	1.7–2.8	0.3–2.2
Distance from TM-derived urban boundary to edge of stable lights at 80% threshold (km)	1.6–5.2	3.6–4.5	1.3–3.0
Distance from TM-derived urban boundary to edge of stable lights at 6% threshold (km)	1.3–8.5	9.3–17.0	3.3–13.0
Shifting of stable lights compared with TM-derived urban boundary	shift to north	shift to north-east	no apparent shift

made over multiple passes of the DMSP platform are most likely the primary source of the exaggeration effects at the lowest thresholds. Given the pattern of Lhasa's urban development during this period (see for example Tibet Heritage Fund 1998), we tend to discount the half-decade temporal difference between our images as an explanation for the northward shift of the lit area.

4.2. *Beijing*

Our land use classification of a 1994 Landsat TM scene of Beijing delineated a contiguous urban area of 663 km^2. The DMSP images show Beijing as a discrete cluster of lights amid a field of four smaller clusters. At the 6% threshold, the stable lights image exaggerates Beijing's urban area by a factor of 5.6; the exaggeration at the 80% threshold is a factor of 2.26. A very high threshold of 97% is required to reduce the lit area to the size of the Landsat-derived urban area. The radiance-calibrated image also shows significant exaggerations: thresholds of $DN \geqslant 1$ and $DN \geqslant 20$ exaggerate the urban area by factors of 9.70 and 2.11, respectively. A moderately high threshold of $DN \geqslant 30$ (radiance $= 1.64^{-8}\,W\,cm^{-2}\,sr^{-1}\,\mu m^{-1}$) matches the TM-derived urban area. Coregistration of the lit areas at optimum thresholds with the TM-derived urban area was better than that seen for Lhasa, although a north-east shift of up to 2.8 km could be discerned. In all cases, the optimal threshold for area also produced the greatest degree of spatial agreement between Landsat TM- and DMSP-derived urban boundaries (see tables 4 and 5).

Of the three cities evaluated here, the 1994 Landsat TM scene we acquired for

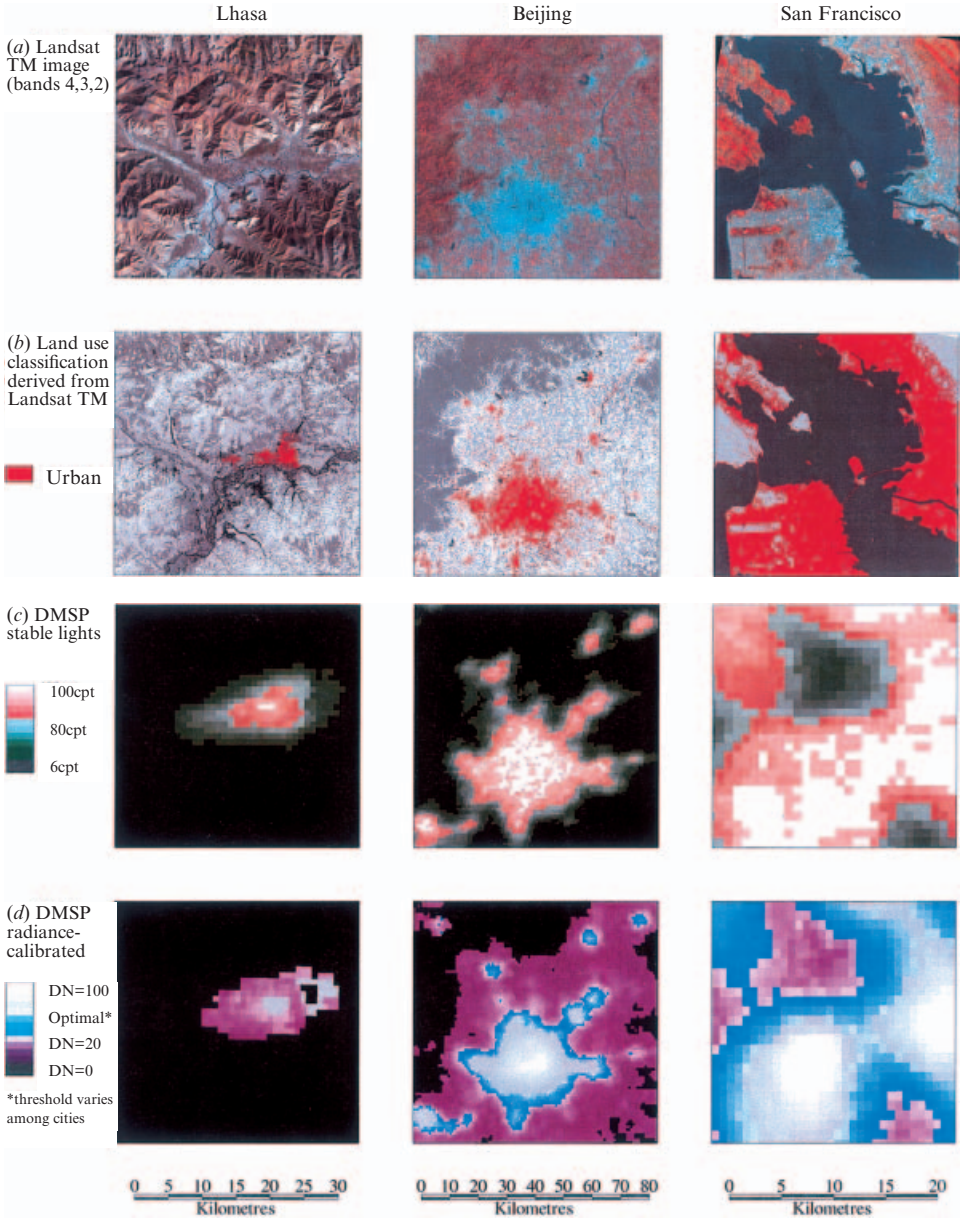

Figure 1. Landsat TM images, urban boundaries and night-time lights images.

Beijing is closest in date to the night-time DMSP imagery—separated by only a month from the initial collection of data for the stable lights composite image. Thus, although Beijing is the most rapidly developing of our three cities, we can discount temporal differences in explaining the exaggeration effects seen in the stable lights image. They may, however, contribute slightly to the effects seen in the radiance-calibrated image. Light reflectance from mountainsides or open water is not likely here. Instead, compounded geo-referencing errors, the intermixture of urban and rural uses along Beijing's fringe, and especially atmospheric interference from Beijing's

Table 2. Confusion matrices for Lhasa, stable lights image.

	At or above threshold	Below threshold	Row total	Omission error
A. Stable lights pixels with light 6% or more of the time (%). Overall accuracy = 96.4%				
Urban	0.5	0.0	0.5	0.0
Not urban	3.6	95.9	99.5	3.6
Column total	4.1	95.9	100.0	
Commission error	88.0	0.0		
B. Stable lights pixels with light 80% or more of the time (%). Overall accuracy = 98.9%				
Urban	0.17	0.3	0.5	66.0
Not urban	0.72	98.7	99.5	0.8
Column total	0.89	99.0	100.0	
Commission error	81.00	0.3		
C. Stable lights pixels with light 88% of the time (%) (optimal threshold at which lit area from DMSP equals urban area from Landsat). Overall accuracy = 99.1%				
Urban	0.08	0.42	0.5	84.0
Not urban	0.50	99.00	99.5	0.5
Column total	0.58	99.42	100.0	
Commission error	86.0	0.4		

Table 3. Confusion matrices for Lhasa, radiance-calibrated image.

	At or above threshold	Below threshold	Row total	Omission error
A. DN $\geqslant$ 1 threshold (%). Overall accuracy = 97.7%				
Urban	0.46	0.04	0.5	8.0
Not urban	2.27	97.23	99.5	2.28
Column total	2.73	97.27	100.0	
Commission error	83.0	0.04		
B. DN $\geqslant$ 20 threshold (%). Overall accuracy = 99.2%				
Urban	0.04	0.46	0.5	92.0
Not urban	0.28	99.2	99.5	0.28
Column total	0.32	99.7	100.0	
Commission error	86.5	0.46		
C. DN $\geqslant$ 19 threshold (%) (optimal threshold at which lit area from DMSP equals urban area from Landsat). Overall accuracy = 99.05%				
Urban	0.05	0.46	0.5	91.0
Not urban	0.47	99.0	99.5	0.48
Column total	0.52	99.48	100.0	
Commission error	91.3	0.46		

notorious air pollution best explain the optimum thresholds used here. Particulates in the air tend to diffuse light emissions. Levels of particulate matter in Beijing's air were measured in 1997 at 370 μm m^{-3}; for comparison, that is three times the peak level recorded in Los Angeles the previous year (World Bank 1997, US Environmental Protection Agency 1996).

The radiance-calibrated image, on the other hand, probably detects the light emitted by agricultural households in the densely populated but non-urban areas outside the city proper. That such low levels of lighting from populated but

Table 4. Confusion matrices for Beijing, stable lights image.

	At or above threshold	Below threshold	Row total	Omission error
A. Stable lights pixels with light 6% or more of the time (%). Overall accuracy = 68.0%				
Urban	6.1	0.67	6.8	10.0
Not urban	31.4	61.8	93.2	34.0
Column total	37.5	62.5	100.0	
Commission error	84.0	1.1		
B. Stable lights pixels with light 80% or more of the time (%). Overall accuracy = 87.8%				
Urban	4.9	1.9	6.8	28.0
Not urban	10.3	82.9	93.2	11.0
Column total	15.2	84.8	100.0	
Commission error	68.0	2.2		
C. Stable lights pixels with light 97% of the time (%) (optimal threshold at which lit area from DMSP equals urban area from Landsat). Overall accuracy = 92.6%				
Urban	3.6	3.2	6.8	47.0
Not urban	4.3	89.0	93.2	4.3
Column total	7.9	92.2	100.0	
Commission error	54.0	3.5		

Table 5. Confusion matrices for Beijing, radiance-calibrated image.

	At or above threshold	Below threshold	Row total	Omission error
A. DN $\geqslant$ 1 threshold (%). Overall accuracy = 41.5%				
Urban	6.65	0.15	6.8	2.2
Not urban	58.35	34.85	93.2	63.0
Column total	65.0	35.0	100.0	
Commission error	90.0	0.4		
B. DN $\geqslant$ 20 threshold (%). Overall accuracy = 88.4%				
Urban	4.6	2.2	6.8	32.0
Not urban	9.4	83.8	93.2	10.0
Column total	14.0	86.0	100.0	
Commission error	67.0	2.6		
C. DN $\geqslant$ 30 threshold (%) (optimal threshold at which lit area from DMSP equals urban area from Landsat). Overall accuracy = 92.8%				
Urban	3.3	3.5	6.8	51.5
Not urban	3.5	89.5	93.2	3.8
Column total	6.8	93.0	100.0	
Commission error	51.5	0.4		

non-urban landscapes is registered in the radiance-calibrated image demonstrates its capability to detect human settlement patterns that would not necessarily be identified in daytime imagery. In the case of the agricultural outskirts of Beijing, electricity use (and presumably night-time lighting) is among the highest in rural China (Skinner 1997), but still low compared with the city proper or with exurban settlements in more developed countries. Hence a moderate threshold is sufficient to distinguish the more brightly lit city from its surrounding countryside.

4.3. *San Francisco*

Based on land use classification of a portion of a 1989 Landsat TM scene focused on San Francisco, we delineated a conterminous urban area of 263 km^2. The DMSP stable lights image at the 6% threshold exaggerated this area by a factor of 3.56, while the exaggeration factor at the 80% threshold was 2.48. For this study area, a threshold of 92% approximated the size of the Landsat TM-derived urban area. In the radiance-calibrated image, thresholds of DN $\geqslant$ 1 and DN $\geqslant$ 20 produced exaggeration factors of 3.00 and 2.34. As seen with Beijing, the latter figure is close to the exaggeration factor of the 80% threshold stable lights. The optimal threshold for the radiance-calibrated image was very high at DN $\geqslant$ 51. Coregistration of the Landsat and DMSP images at optimum thresholds was reasonably good, with shifts of up to 2.2 km but no directional pattern. Spatial agreement of urban areas between the DMSP and Landsat sources increased as the area-optimized thresholds were approached (see tables 6 and 7).

Temporal differences would not appear to explain the differences seen here. The Landsat TM imagery we acquired for San Francisco predates the night-time DMSP stable lights imagery by five years, but there has been no significant change in the urban boundary within our study area in that time. Image coregistration at the optimal thresholds is the best of our three study sites. This allows us to attribute much of the exaggeration at lower stable lights thresholds to the effect of random walk geo-referencing errors that accumulate when the stable lights composite image is generated. Reflectance from non-urban surfaces, particularly the San Francisco Bay, is responsible for much of the remaining exaggeration effect. The stable lights image shows much of the Bay between San Francisco and Oakland as lit even at the 100% threshold, reminding us that light was reflected from this water surface to the DMSP sensor on *every* orbit. Applying the high threshold of DN $\geqslant$ 51 to the radiance-calibrated image helps to overcome this effect.

Table 6. Confusion matrices for San Francisco, stable lights image.

	At or above threshold	Below threshold	Row total	Omission error
A. Stable lights pixels with light 6% or more of the time (%). Overall accuracy = 28.7%				
Urban	27.9	0.0	27.9	0.0
Not urban	71.3	0.8	72.1	99.0
Column total	99.2	0.8	100.0	
Commission error	72.0	0.0		
B. Stable lights pixels with light 80% or more of the time (%). Overall accuracy = 57.3%				
Urban	27.3	0.5	27.8	1.8
Not urban	42.2	30.0	72.2	58.0
Column total	69.5	30.5	100.0	
Commission error	61.0	1.6		
C. Stable lights pixels with light 92% of the time (%) (optimal threshold at which lit area from DMSP equals urban area from Landsat). Overall accuracy = 68.0%				
Urban	25.4	2.5	27.9	9.0
Not urban	29.3	42.8	72.1	41.0
Column total	54.7	45.3	100.0	
Commission error	54.0	5.0		

Table 7. Confusion matrices for San Francisco, radiance-calibrated image.

	At or above threshold	Below threshold	Row total	Omission error
A. DN $\geqslant$ 1 threshold (%). Overall accuracy = 44.3%				
Urban	27.9	0.0	27.9	0.0
Not urban	55.7	16.4	72.1	77.0
Column total	83.6	16.4	100.0	
Commission error	66.7	0.0		
B. DN $\geqslant$ 20 threshold (%). Overall accuracy = 61.5%				
Urban	27.4	0.5	27.9	1.8
Not urban	38.0	34.1	72.1	53.0
Column total	65.4	34.6	100.0	
Commission error	58.0	14.4		
C. DN $\geqslant$ 51 threshold (%) (optimal threshold at which lit area from DMSP equals urban area from Landsat). Overall accuracy = 79.7%				
Urban	17.0	10.9	27.9	39.0
Not urban	9.4	62.7	72.1	13.0
Column total	26.4	73.6	100.0	
Commission error	36.0	14.8		

5. Discussion and conclusions

These results demonstrate that, for cities at different levels of development, quite different thresholds are required when using DMSP night-time lights imagery to delineate areas that approximate the urban areas seen in daytime Landsat TM imagery. Higher radiance thresholds are required with higher levels of economic development. In fact, non-urban areas on the outskirts of San Francisco and Beijing show higher levels of light radiance than the urban core of Lhasa. This substantiates the initial premise of the recent research on DMSP imagery that the intensity of cities' night-time lighting is largely proportional to their population and level of economic development.

We have shown that appropriate radiance thresholds can be used to distinguish the lights of urban areas from surrounding rural settlements and from the exaggeration effects inherent in the DMSP radiance-calibrated imagery. While this paper demonstrates that it is not possible to settle upon a single radiance threshold that can be used to delineate urban boundaries across the board, it leaves open the possibility that thresholds can be chosen for cities at comparable levels of development and urbanization. Further applications of this technique will be required to demonstrate whether the optimal radiance thresholds we determined for Lhasa, Beijing and San Francisco produce optimal elsewhere. We suggest repeating this method to compare TM- and DMSP-derived urban boundaries for more cities at similar levels of economic development.

Thresholds based on the stable lights are more problematic, especially when compared across cities at different levels of development. Our optimal stable lights threshold for San Francisco, 92%, is higher than the values of 82% and 89% that Imhoff *et al.* (1997a and b, respectively) suggest as good measures of urban extent in the continental US, let alone the 80% threshold applied by Sutton *et al.* (1999a) elsewhere. For Beijing, we found an even higher threshold of 97% to be optimal. This threshold is much higher than any that has been suggested for detecting urban

populations elsewhere. Even Lhasa, the least developed city represented here, required a stable lights threshold (88%) at the high end of the range previously reported for the US. These findings are difficult to interpret and thresholding for stable lights image remains, as Sutton *et al.* (1999a) put it, an *ad hoc* procedure. Now that the radiance-calibrated DMSP image is available, we find that its representation of the brightness of cities is a more readily interpretable source of data on urban boundaries than the stable lights dataset.

In parting, we note that DMSP night-time imagery provides a different perspective on urban land use than daytime imagery. This calls into question how 'urban' should be defined in remote sensing studies. For example, are large parklands amidst urban areas (i.e. Golden Gate Park or Mount Tamalpais in our San Francisco study area) or mixed agricultural–industrial zones (as on the outskirts of Beijing) to be considered urban or not? In our Landsat analysis, the trees and meadows of Golden Gate Park were classified as non-urban, even though the social use of the park as a whole is urban. Furthermore, unlike 'natural' green areas, the park's lit pathways and street lights contribute to the light emissions of the city. Similarly, light from the outskirts of Beijing, which are dominated by agricultural fields in our Landsat TM image, reveals that these periurban areas have hidden 'urban' characteristics. By revealing the range of intensities of night-time lights, the DMSP radiance-calibrated image offers a unique and useful perspective for monitoring the extent and level of urbanization at a global scale.

Acknowledgments

Henderson and Yeh share senior co-authorship of this paper. Image processing facilities and Landsat imagery of San Francisco and Beijing were provided by the Center for Assessment and Monitoring of Forest and Environmental Resources (CAMFER) at the University of California, Berkeley, and partly supported by a National Aeronautics and Space Administration (NASA) land cover and land use change grant and a National Science Foundation of China grant (49825511) to Gong. We thank Dr Paul Sutton, Dr Ye Qi and two anonymous reviewers for thoughtful comments on an earlier draft.

References

Alexander, A., and De Azevedo, P., 1998, *The Old City of Lhasa* (Berlin: Tibet Heritage Fund).

Brown, L. R., 1995, *Who Will Feed China?: Wake-up Call for a Small Planet* (New York: W. W. Norton & Company).

CIESIN (Center for International Earth Science Information Network), 1996, Digital chart of China, 1:1M. Available online: http://sedac.ciesin.org/china/geogmap/dcchina/dcchina.html.

Coulter, J., and Ivory, P., 1982, The rural–urban dichotomy in China: a case study of the mid-Yellow River region using remote sensing data. *Australian Journal of Chinese Affairs*, **7**, 37–53.

Dickenson, T. E., 1975, Agriculture in the future and its implications for land-use planning. University of California, Division of Environmental Studies, Davis, CA, USA.

Ding, Y., Elvidge, C. D., and Lunetta, R. S., 1998, Survey of multispectral methods for land cover change detection analysis. In *Remote Sensing Change Detection: Environmental Monitoring Methods and Applications*, edited by C. D. Elvidge and R. S. Lunetta (New York: Sleeping Bear Press), pp. 21–39.

Elvidge, C. D., 2000b, Radiance calibration of DMSP-OLS low-light imaging data of human settlements (CD-ROM). US Department of Commerce, National Oceanographic and Atmospheric Administration.

Elvidge, C. D., and Baugh, K. E., 1998, Stable lights and radiance-calibrated lights of the world (CD-ROM). US Department of Commerce, National Oceanographic and Atmospheric Administration.

Elvidge, C. D., Baugh, K. E., Hobson, V. R., Kihn, E. A., Kroehl, H. W., Davis, E. R., and Coceros, D., 1997a, Satellite inventory of human settlements using nocturnal radiation emissions: a contribution for the global toolchest. *Global Change Biology*, **3**, 387–295.

Elvidge, C. D., Baugh, K. E., Kihn, E. A., Kroehl, H. W., and Davis, E., 1997b, Mapping city lights with night-time data from the DMSP operational linescan system. *Photogrammetric Engineering and Remote Sensing*, **63**, 727–734.

Elvidge, C. D., Baugh, K. E., Hobson, V. R., Kihn, E. A., and Kroehl, H. W., 1998, Detection of fires and power outages using DMSP-OLS data. In *Remote Sensing Change Detection*, edited by R. S. Lunetta and C. D. Elvidge (Chelsea, MI, USA: Ann Arbor Press).

Elvidge, C. D., Baugh, K. E., Dietz, J. B., Bland, T., Sutton, P. C., and Kroehl, H. W., 1999, Radiance calibration of DMSP-OLS low-light imaging data of human settlements. *Remote Sensing of Environment*, **68**, 77–88.

Imhoff, M. L., Lawrence, W. T., Stutzer, D. C., and Elvidge, C. D., 1997a, A technique for using composite DMSP/OLS 'city lights' satellite data to accurately map urban areas. *Remote Sensing of Environment*, **61**, 361–370.

Imhoff, M. L., Lawrence, W. T., Elvidge, C., Paul, T., Levine, E., Prevalsky, M., and Brown, V., 1997b, Using night-time DMSP/OLS images of city lights to estimate the impact of urban land use on soil resources in the U.S. *Remote Sensing of Environment*, **59**, 105–117.

Krohe, J. Jr., 1986, Buy now, save later: a farmland proposal. *Planning* (November).

Lo, C. P., and Welch, R., 1977, Chinese urban population estimates. *Annals of the Association of American Geographers*, **67**(2), 246–253.

Lo, C.-P., Pannell, C. W., and Welch, R., 1977, Land use changes and city planning in Shenyang and Canton. *The Geographical Review*, **67**, 268–283.

NOAA (US National Oceanic and Atmospheric Administration), 1999, Defense Meteorological Satellite Program. Available online: http://www.ngdc.noaa.gov/dmsp.

NOAA (US National Oceanic and Atmospheric Administration), 2001, NOAA/NASA Pathfinder AVHRR land data sets. Available online: http://daac.gsfc.nasa.gov/DATASET_DOCS/avhrr_dataset.html.

Skinner, G. W., 1997, China-A data set. University of California Department of Anthropology, Davis, CA, USA.

Sutton, P., 1997, Modeling population density with night-time satellite imagery and GIS. *Computers, Environment, and Urban Systems*, **21**, 227–244.

Sutton, P., Roberts, D., Elvidge, C. D., and Meij, H., 1997, A comparison of night-time satellite imagery and population density for the continental United States. *Photogrammetric Engineering and Remote Sensing*, **63**, 1303–1313.

Sutton, P., Roberts, D., Elvidge, C., and Miej, H., 1999a, Census from heaven: an estimate of the global human population using night-time satellite imagery. Paper presented at the Western Regional Science Association annual meeting, Ojai, California, USA, February 1999.

Sutton, P., Roberts, D., Leskow, J., and Elvidge, C., 1999b, Modeling urban population density with night-time satellite imagery. Unpublished manuscript, University of Denver Department of Geography, USA.

Tibet Heritage Fund, 1998, *Tibetan Old Buildings and Urban Development in Lhasa* (Berlin: Verlag Freie Kultur Aktion).

US Environmental Protection Agency, 1996, National air quality and emissions trends report. Document Number 454/R-97-013, US EPA Office of Air Quality Planning and Standards. Available online: http://www.epa.gov/oar/aqtrnd96/toc.html.

World Bank, 1997, World development indicators. International Bank for Reconstruction and Development, Washington, DC, USA.